

3D Modeling of Dynamic Facial Expressions for Face Image Analysis and Synthesis

Yu Zhang¹, Eric Sung¹ and Edmond C. Prakash²

¹School of Electrical and Electronic Engineering, ²School of Computer Engineering
Nanyang Technological University, Singapore 639798

Abstract

In this paper we propose a physically-based 3D dynamic facial model based on anatomical knowledge for facial image analysis and synthesis. The 3D face model has a three dimensional structure of anatomically-motivated facial skin and muscles. Facial skin is modeled by a nonlinear spring frame which can simulate the elastic dynamics of real facial skin. Three kinds of muscle models are developed to simulate real facial muscle contraction. Based on FACS (Facial Action Coding System), facial expressions are generated by the contraction of a set of facial muscles. Lagrangian mechanics governs the dynamics, dictating the deformation of facial surface in response to muscular forces. Experimental results show our physically-based model can dynamically create the flexible and realistic expressions which can be matched with real human examples. Using our system, we can effectively analyze the relationship between facial surface deformation and the activation of underlying facial muscles. We also indicate how our model can be used for face and facial expression recognition.

1 Introduction

1.1 Background

The human face is an important and complex communication channel. It is a very familiar and sensitive object of human perception. The complexity and expressions of human face makes it a difficult subject for automated visual interpretation. It has attracted attention in several disciplines including psychology, computer vision and computer graphics. In recent years, facial image analysis and synthesis have been used in such diverse fields as model-based video coding[1], advanced man-machine interface agents and avatars[9], facial expression recognition[5][19] and facial surgery planning[8].

At present, most methods of facial images synthesis are based on the 3D facial models which are constructed by polygons. A number of methods have been proposed to deform a facial model to generate facial

expressions. The most intuitive and still widely used approach is key-frame interpolation. Key-frames, or basic expressions in 3D are defined at different moments in the animated sequence. Intermediate expressions are simply interpolated between two successive basic expressions. Parke's pioneering work [13] is based on this method. This kind of modeling method can effectively create facial images in a short amount of computational time, and can be used for applications which require the real-time performance rather than the accurate facial modeling.

The parameterized facial models developed in [2][3][14][15] are the extensions of the previous key-frame interpolation face model. The parameterized model is experimentally derived to represent the visible surface features of the face based on observation and a general understanding of the underlying structures. It makes use of local region interpolation, geometric transformations, and mapping techniques to manipulate the feature of the face. The desire was to create an encapsulated model which would generate a wide range of faces and facial expressions based on a fairly small set of input control parameters. But due to the lack of knowledge about facial anatomy, it is not appropriate for applications requiring close fidelity to real facial motion and expression.

Another different approach is the free-form deformation facial modeling [6][7][12]. The idea for this method, is not to exactly simulate the detailed facial anatomy but rather to develop models with only a few control parameters that emulate the basic face muscle actions. To simulate the facial muscle actions, surface regions corresponding to anatomical regions of the desired muscle actions are defined. A parallelepiped control lattice is defined around each muscle region. The facial skin deformations are simulated by interactively displacing the lattice control points and by changing the weight assigned to each control point.

The more sophisticated facial modeling method is the physically-based approach. It is based on the fact that the actual facial expressions are generated by the

dynamics of the facial muscles which are under the skin. To date, no facial models based on the complete detailed facial anatomy have been reported. However, several models have been developed that are based on simplified models of facial bone structure, muscles, connective tissue, and skin [8][11][17]. In [8], Rolf Koch et al. presented an approach for surgical planning and prediction of facial shape after craniofacial and maxillofacial surgery for patients with facial deformities using finite element models. Although the system can achieve high performance, however, a quantitative analysis of the relationship between facial muscles and facial skin deformation has not been done in detail. And the large computational expense prevents its usage in real-time application. Lee et al. [11] used a laser scanner to obtain range and color data for model fitting, and produced physically-based model capable of animation. However, his model only has one kind of facial muscle, which limits the scope of expression animation.

1.2 Motivation

Because face is highly deformable, particularly around the forehead, eyes, cheeks and mouth, these deformations convey a great deal of meaningful information. It is believed that a good foundation for facial expression recognition and analysis is the anatomy of the face, especially the arrangements and actions of the primary facial muscles. Therefore developing a detailed 3D model of the human face and its musculature and then incorporate it for facial image analysis and synthesis is a promising way forward. This approach requires a realistic 3D facial model sophisticated enough to accurately reproduce the various nuances of facial structure and motion.

In this paper, we propose a 3D physical face model from the anatomical perspective, which has a three dimensional structure of the muscles and skin. The skin model is constructed by using the nonlinear spring frames which can simulate the elastic dynamics of real facial skin. The facial expressions are synthesized in a way similar to the one in real human face. Three kinds of muscle models are developed to emulate facial muscles contraction. When muscles contract, by solving the dynamic equation for each skin node in the facial surface, we can obtain flexible and realistic facial expressions.

1.3 Preview

The remainder of this paper is organized as follows: In Section 2, the physically-based facial skin model is presented. Section 3 presents our dynamic muscle models. Section 4 illustrates the motion dynamics and numerical simulation of our facial model. The imple-

mentation and results are explained in Section 5. In Section 6, we discuss the application of this 3D facial model to face and facial expression recognition. We finish by presenting some conclusions and future work.

2 Physical facial skin model

Experimental results have shown that living biological tissue has a non-linear, viscoelastic stress-strain relationship as shown in Fig. 1. Under low stress, dermal tissue offers very low resistance to stretch, but under greater stress it resists stretch much more markedly. The history of strain affects the stress, which means that the stress-strain relations in the loading and unloading processes are different. Each branch of a specific cyclic process can be described by a non-linear pseudo-elastic function. Since the difference is insignificant, we approximate the non-linear relationship by a biphasic curve illustrated in Fig. 1.

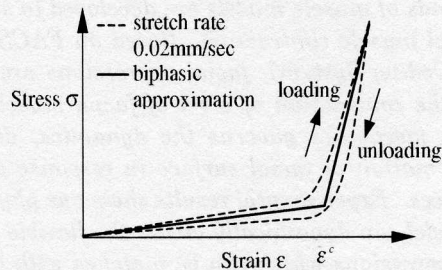


Figure 1: Stress-strain relationship of facial tissue

Our facial model is constructed by polygon meshes. It consists of 702 vertices and 1284 polygons, with finer polygons over the highly curved and/or highly articulate regions of face, such as the eyes and mouth, and larger polygons elsewhere, such as cheek and forehead. Fig. 2 shows our 3D face model, where (a) is a wire frame face, and (b) is the smoothly shaded face. In order to physically simulate the deformation of the facial skin tissue, we use the mechanical law of particles. The motion of a particle is defined by its physical nature and by the position of other objects and particles in its neighborhood. In our specific case, we only consider the representation of facial surface. The facial surface is composed by a set of particles with mass density m . Their behavior is determined by their interaction with the other particles that define the face surface. To simulate elastic effects of facial skin tissue, we have used concepts from the theory of elasticity [10]. We connected each face skin point with its neighbors by nonlinear springs whose elastic property is represented by the biphasic curve shown in Fig. 1.

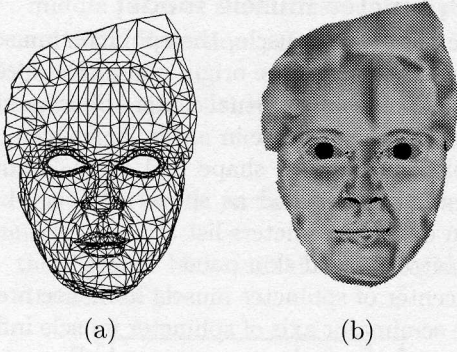


Figure 2: (a) Wire frame face model (b) Smoothly shaded face model

Suppose an arbitrary skin mesh point \mathbf{x}_i is connected with mesh point \mathbf{x}_j by the spring j . The spring stiffness k_{ij} and rest length r_j^r . The current length of the spring is $r_j = \|\mathbf{x}_j - \mathbf{x}_i\|$. Considering that the elastic force produced by a spring j over a mass point i is

$$q_{ij} = k_{ij}\varepsilon_j u_{ij} \quad (1)$$

where

$$\varepsilon_j = r_j - r_j^r \quad (2)$$

$$k_{ij} = \begin{cases} k_l & \varepsilon_j \leq \varepsilon^c \\ k_h & \varepsilon_j > \varepsilon^c \end{cases} \quad (3)$$

$$u_{ij} = \frac{\mathbf{x}_j - \mathbf{x}_i}{r_j} \quad (4)$$

the low-strain stiffness k_l is smaller than the high-strain stiffness k_h . Like real skin tissue, the biphasic spring is readily extendible at low strains, but exerts rapidly increasing restoring stresses after exceeding a strain threshold ε^c . The total elastic force applying on skin point \mathbf{x}_i due to springs which connect it to its neighbors is

$$Q_i = \sum_{j \in \mathcal{N}_i} q_{ij} \quad (5)$$

where \mathcal{N}_i is the index set of neighboring nodes.

3 Facial muscle model

The muscles of the face are commonly known as the muscles of facial expression. The muscles of facial expression are superficial, they are mostly attached to both the skull and the facial tissue. One end of the facial muscle attached to skull is generally considered the origin while the other one is the insertion. Normally, the origin is the fixed point, and the insertion is where the facial muscle performs its action. Muscles are bundles of muscle fibers working in unison. The

shape of the fiber bundle determines the muscle type and its functionality. In human face, a wide range of muscle types exist: rectangular, triangular, sheet, linear, sphincter [18]. There are three main types of facial muscles incorporated in our face model:

Linear muscle: It consists of a bundle of fibers that share a common emergence point in bone and pulls in an angular direction. One of the examples is the zygomaticus major which attaches to and raises the corner of the mouth.

Sphincter muscle: It consists of fibers that loop around facial orifices and can draw towards a virtual center; an example is the orbicularis oris, which circles the mouth and can pout the lips.

Sheet muscle: It is a broad, flat sheet of muscle fiber strands without a localized emergency point. The most obvious example is the lateral frontalis, one of the forehead muscles that raise the outer portion of the eyebrows.

3.1 Linear muscle model

On contraction, facial regions close to the skin insertion point of a muscle are affected. The effect of facial muscle contraction is to pull the surface from the area of the muscle insertion point to the muscle attachment point. The muscular influence decreases with both the decreasing of the distance from muscle attached point l_{ji} and increasing of the angle from muscle vector φ_{ji} . It is assumed that there is zero influence at the point of muscle attachment to the bone (m_j^A) and that maximum influence occurs at the muscle insertion point (m_j^I). Consequently, a fall-off of the muscle force is dissipated through the adjoining tissue in the influence area of the muscle. Fig. 3 illustrates the linear muscle model with the following definitions:

\mathbf{x}_i : arbitrary facial skin point

m_j^A : attachment point of linear muscle j at the skull

m_j^I : insertion point of linear muscle j at the facial skin

R_j : the maximum radius of influence

φ_j : the maximum angle of influence

φ_{ji} : the angle between muscle vector and \mathbf{x}_i

l_{ji} : the distance between muscle attachment point m_j^A and skin point \mathbf{x}_i

l_{ji} is calculated as:

$$l_{ji} = \|\mathbf{m}_j^A - \mathbf{x}_i\| \quad (6)$$

l_{ji} and φ_{ji} weight the influence of muscle j at vertex i separately for length factor λ_{ji} and angular factor γ_{ji} :

$$\lambda_{ji} = \frac{l_{ji}}{\|\mathbf{m}_j^A - \mathbf{m}_j^I\|} \quad (7)$$

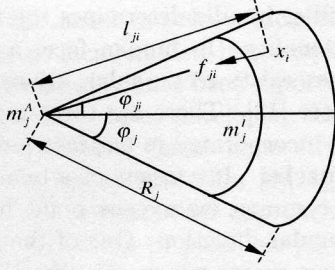


Figure 3: Linear muscle model

$$\gamma_{ji} = \frac{\varphi_{ji}}{\varphi_j} \quad (8)$$

λ_{ji} defines the longitudinal distance of vertex i to muscle j normalized to values between 0 and 1. A value around 0, or 1 signifies that vertex i lies close to the muscle attachment point, or close to the insertion point, respectively. The influence of the muscle j increase with λ_{ji} . γ_{ji} is defined in $[0,1]$ and represents the latitude distance between vertex i and muscle j . φ_j defines maximum influence angle. Increasing γ_{ji} results in decreasing the influence of muscle j . The muscular force applied at vertex i can be computed as

$$\vec{f}_{ji} = \alpha_L \Theta_1(\lambda_{ji}) \Theta_2(\gamma_{ji}) \nu_{ji} \quad (9)$$

where

$$\nu_{ji} = \frac{(m_j^A - \mathbf{x}_i)}{\|m_j^A - \mathbf{x}_i\|} \quad (10)$$

In equation(9), α_L is muscular force scaling factor. Function Θ_1 scales the muscle force according to the length ratio, while Θ_2 scales the muscle force according to the angular ratio γ_{ji} at node \mathbf{x}_i . We define

$$\delta_j = \frac{R_j}{\|m_j^A - m_j^I\|} \quad (11)$$

and

$$\Theta_1(\lambda_{ji}) = \begin{cases} \cos((1 - \lambda_{ji}^{\eta_j}) \cdot \frac{\pi}{2}) & 0 \leq \lambda_{ji} \leq 1 \\ \cos((\frac{\lambda_{ji}^{\eta_j} - 1}{\delta_j^{\eta_j} - 1}) \cdot \frac{\pi}{2}) & 1 < \lambda_{ji} \leq \delta_j \end{cases} \quad (12)$$

$$\Theta_2(\gamma_{ji}) = \cos(\varphi_j \gamma_{ji}) \cos(\gamma_{ji} \cdot \frac{\pi}{2}) \quad 0 \leq \gamma_{ji} \leq 1 \quad (13)$$

The constant η_j defines the strength of muscle j . A decrease in the value of η_j increases the muscle influence along the longitude.

3.2 Sphincter muscle model

Unlike the linear muscle, the sphincter muscle attaches to skin both at the origin and at the insertion, and contracts around a virtual center. Because sphincter muscles do not behave in a regular fashion, it can be modeled in elliptical shape and can be simplified to a parametric ellipsoid as shown in Fig. 4. The definition of the parameters list are:

- \mathbf{x}_i : arbitrary facial skin point
- o : epicenter of sphincter muscle influence area
- a : the semimajor axis of sphincter muscle influence area
- b : the semiminor axis of sphincter muscle influence area

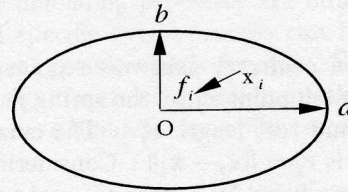


Figure 4: Sphincter muscle model

The muscular force applied at vertex i is computed as

$$\vec{f}_i = \alpha_s \Theta(r_i) \nu_i \quad (14)$$

where α_s is sphincter muscular force scaling factor and

$$\nu_i = \frac{(o - \mathbf{x}_i)}{\|o - \mathbf{x}_i\|} \quad (15)$$

$$\Theta(r_i) = \cos((1 - d_i) \cdot \frac{\pi}{2}) \quad 0 \leq r_i \leq 1 \quad (16)$$

in equation (16)

$$d_i = \frac{\sqrt{y_i^2 a^2 + x_i^2 b^2}}{ab} \quad (17)$$

3.3 Sheet muscle model

Sheet muscle consists of strands of fibers which lie in flat bundles. A sheet muscle neither emanates from a point source, nor contracts to a localized node. In fact, it is a series of almost-parallel fibers spread over an rectangle area. Fig. 5 illustrates the sheet muscle model. Two points m_j^{A1} and m_j^{A2} specify the attachment line of the sheet muscle. m_j^{Ac} is the middle point of m_j^{A1} and m_j^{A2} . Similarly, the points m_j^{I1} and m_j^{I2} specify the insertion line of the sheet muscle, and m_j^{Ic} is the middle point of m_j^{I1} and m_j^{I2} .

- \mathbf{x}_i : arbitrary facial skin point
- m_j^{A1} and m_j^{A2} : attachment points defining attachment line of sheet muscle j

m_j^{Ac} : middle point of sheet muscle attachment line
 m_j^{I1} and m_j^{I2} : insertion points defining insertion line of sheet muscle j
 m_j^{Ic} : middle point of sheet muscle insertion line
 L_j : the length of the rectangle zone influenced by sheet muscle
 W_j : the width of the rectangle zone influenced by sheet muscle
 l_{ji} : the distance between skin point x_i and sheet muscle attachment line

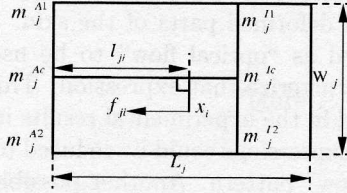


Figure 5: Sheet muscle model

In the sheet muscle model, the muscular force applied at vertex i is calculated as

$$\vec{f}_{ji} = \alpha_{st} \Theta(\lambda_{ji}) m_j \quad (18)$$

where α_{st} is sheet muscular force scaling factor and

$$m_j = \frac{(m_j^{Ac} - m_j^{Ic})}{\|m_j^{Ac} - m_j^{Ic}\|} \quad (19)$$

$$\Theta(\lambda_{ji}) = \begin{cases} \cos((1 - \lambda_{ji}^{\eta_j}) \cdot \frac{\pi}{2}) & 0 \leq \lambda_{ji} \leq 1 \\ \cos((\frac{\lambda_{ji}^{\eta_j} - 1}{\delta_j^{\eta_j} - 1}) \cdot \frac{\pi}{2}) & 1 < \lambda_{ji} \leq \delta_j \end{cases} \quad (20)$$

in the formula (20), η_j is the sheet muscle strength factor and

$$\lambda_{ji} = \frac{l_{ji}}{\|m_j^{Ac} - m_j^{Ic}\|} \quad (21)$$

$$\delta_j = \frac{L_j}{\|m_j^{Ac} - m_j^{Ic}\|} \quad (22)$$

4 Dynamics of the 3D facial model

The simulation of facial expressions requires a mapping of the desired facial expression into facial muscle activation. The Facial Action Coding System (FACS) was developed by Ekman and Friesen [4] for this purpose. FACS describes the set of all possible basic actions performable on the human face. Each basic action is called an Action Unit or AU. Such actions are based on the anatomy of the face, each being caused by either a single muscle or a small set of closely related muscles. FACS identifies 66 AUs which, separately or in various combinations, are capable of characterizing any human expression[4]

FACS has been used as a basis in our system for generation of facial expressions. Various facial expressions are created by the combination of the contraction of certain facial muscles. In order to generate facial expressions, we select 10 kinds of major functional facial muscles and simulate their contractions by using the three types of muscle models. Fig.6 illustrates the positions of these muscles in the 3D face. When the muscles contract, the facial skin points that are in the influence area of the muscle model are displaced to their new positions. As a result, the facial skin points not influenced by the muscle contraction are in an unstable state, and unbalanced elastic forces propagate through the mass-spring system to establish a new equilibrium state.

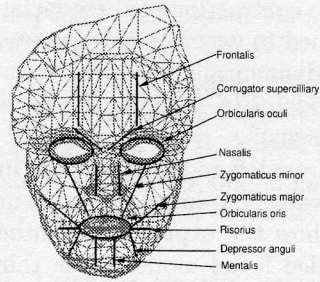


Figure 6: Major facial muscles definition

Applying external forces to the deformable facial model yields realistic dynamics. In our face model, the net externally applied forces include the muscle force and the gravitational force. Based on the Lagrangian dynamics, the deformable facial model equations of motion can be expressed in 3D vector form by the second-order ordinary differential equations:

$$m_i \frac{\partial^2 \vec{x}_i}{\partial t^2} + c_i \frac{\partial \vec{x}_i}{\partial t} + Q_i = \sum_{j \in \mathcal{N}_i} f_{ij}(\vec{x}_i) + m_i g \quad (23)$$

$$\vec{x}_i = [x_i(t), y_i(t), z_i(t)] \quad (24)$$

where m_i is the nodal mass, c_i is the velocity-dependent damping coefficient that controls the rate of dissipation of kinetic energy which eventually brings facial mesh to rest, g is a gravitational constant, Q_i is the total elastic force on node i due to springs connecting it to neighboring nodes, and f_{ji} is the individual muscle force applied on node i .

The solution of the nodal displacement, velocity and acceleration at time $t + \Delta t$ can be obtained by numerical integration. In the simulation, we use a second-order Runge-Kutta method [16] to integrate ordinary differential equations. We have chosen this

method because it is more accurate and stable than Euler's method while retaining an acceptable time of execution.

5 Experimental Results

To illustrate the applications of the methods described, we have implemented a facial modeling system. It runs on a SGI Power Onyx/RE2, R10000, 195MHz, 512MB. In the experiment, we used the physically-based face model to create primary facial expressions. They are sadness, anger, happiness, surprise and disgust. In each expression simulation, we select the major functional muscles according to the Action Unit of the FACS. For instance, sadness is represented by AU1+AU15 in the FACS, the associated facial muscles are frontalis and depressor anguli. By simulating the contraction of these facial muscles, the skin is deformed to generate this expression. The expressions are dynamically produced by our physically-based face model. Fig. 7 shows the movement of face model on "Disgust".

In Fig. 8, from left to right, the first images are the typical expressions produced by a real man. The second images show the expressions synthesized by the OpenGL shaded facial model. The third ones illustrate the wire frame model with the facial muscles (red lines) involved to generate this expression. The images on the right are the 3D motion tracking of the mesh nodes on the face model, which correspond to each synthesized facial expression respectively. In the motion tracking, the motionless vertices are in blue and the colorful trajectories illustrate the motion of the displaced vertices during expression generation process from blue at the first frame to red at the last frame. Comparing the first column of images with the second ones in Fig. 8, we can see that the expressions generated by our physically-based facial model is so realistic as that of the real person.

6 Application to face and facial expression recognition

In section 5 we show that our physically-based facial model can generate flexible facial images. One reason is that our facial model takes anatomical knowledge into account and considers the physical properties such as mass distribution, elasticity and viscosity of facial skin. It approximates not only the facial shape, but also the actual mechanism of the process that generate facial expressions. The biggest advantage of our expression modeling system is that it can analyze the relationship between the facial skin deformation and the inside state, which is determined by facial muscle contractions.

Face recognition from a single intensity or color image is greatly affected by pose, lighting conditions, artifacts and different facial expressions. We address the last case, how can we equate an image of a person's expressionless face to that of the same person with say a smile? For that matter, how can we tell that the person is smiling? Our approach is to fall back on computer graphics and model a realistic human head with the ability to generate realistic expressions. With such a model, we can use it in various ways. Tracking of the dynamics of an expression yields a sort of velocity flow of deformed parts of the skin. This could be interpreted as "optical flow" to be used as templates to characterize that expression. This has been demonstrated in the experimental results in section 5. Hence facial expressions could be reduced to templates of "optical flow" pattern. Another possible way is to obtain range data from active light source and insert the skin and muscle structure into it. This makes the 3D range data "come alive". It is thus endowed with trained sets of expressions generation. Not only can we predict the person's face from different pose but also with different expressions as well. This provides a powerful alternative approach to predict different views from a single image. A final challenge is to fit our generic face model to a specific person's face given only a image of that person. This final approach is still under study.

7 Conclusion

This paper has proposed a physically-based facial model constructed from anatomical perspective. Three kinds of muscle models are developed to simulate real facial muscle contraction. Skin model is constructed by a nonlinear spring frame which can simulate the elastic dynamics of real facial skin. Based on the Lagrangian dynamics, facial tissue is deformed as the muscle force applying on it. Using our facial model, we can generate flexible and realistic expressions. Our dynamic facial model enables us to predict deformation of the facial shape caused by emotions. We have also indicated how our face model can be applied to face and facial expression recognition.

For the future work, we will extend the one-layer skin model to the multi-layer structure which fully simulate the real skin tissue. In order to accurately simulate the articulation of the chin, the skull model will also be included. Moreover, we will research the relationship between facial expressions and the internal facial structure (muscle and skull) in addition to creating realistic facial images.

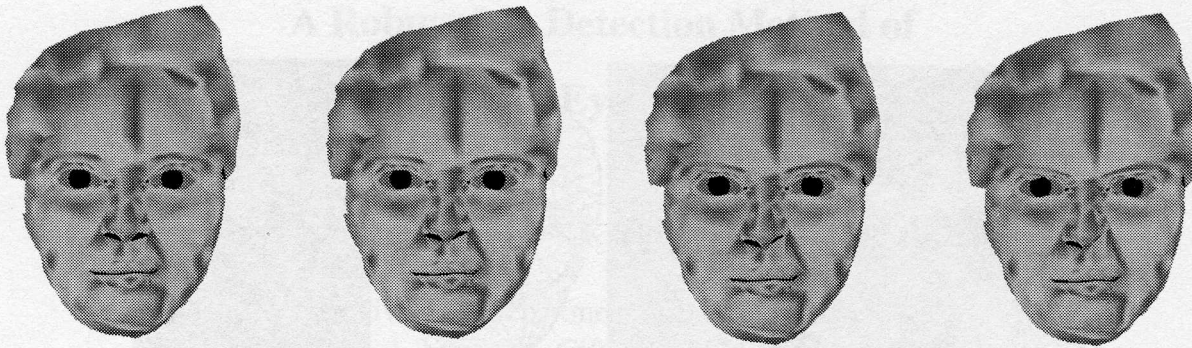
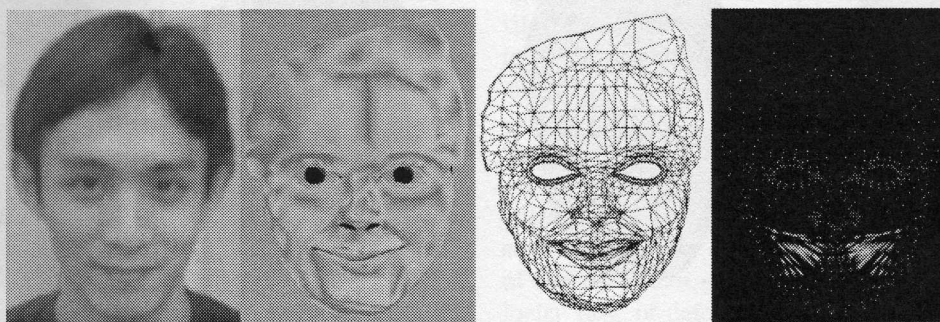


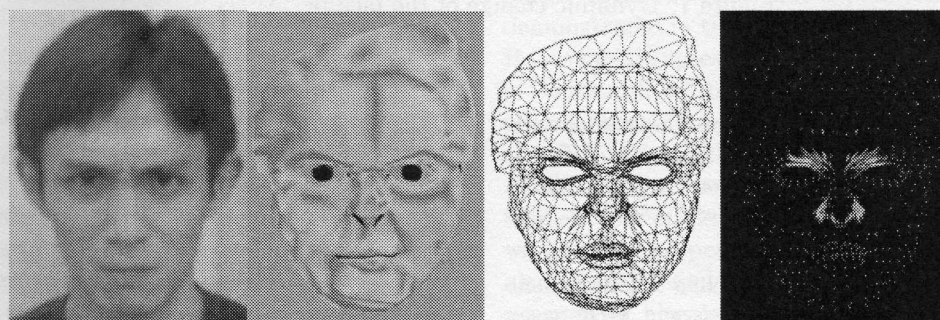
Figure 7: Dynamic change of the face in "Anger"

References

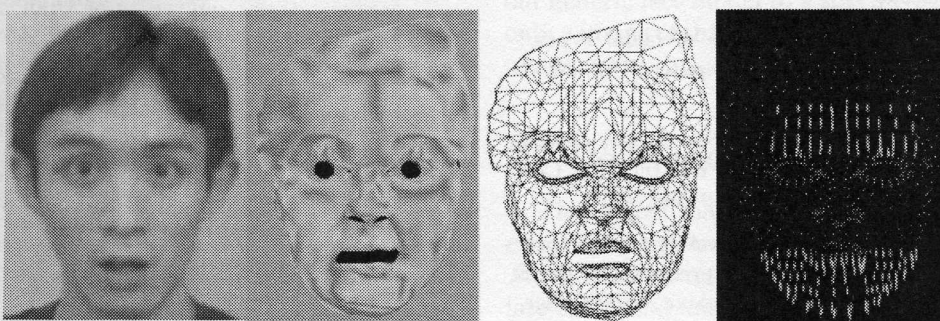
- [1] Chang S. Choi, Kiyoharu, Hiroshi Harashima, and Tsuyoshi Takebe, "Analysis and synthesis of facial image sequences in model-based image coding," *IEEE Tran. Circuits and Systems for Video Technology*, volume 4, pages 257-275. June 1994.
- [2] M. Cohen and D. Massaro, "Modeling coarticulation in synthetic visual speech," *Models and Techniques in Computer Animations*, pages 141-155, Springer-Verlag, Tokyo, 1993.
- [3] S. DiPaola, "Extending the range of facial types," *Journal of Visualization and Computer Animation*, 2(4): 129-131, 1991.
- [4] P. Ekman and W. V. Friesen, *Facial Action Coding System*, Consulting Psychologists Press Inc., 577 College Avenue, Palo Alto, California 94306, 1978.
- [5] I. Essa and A. Pentland, "Coding, analysis, interpretation and recognition of facial expressions," *IEEE Tran. Pattern Analysis and Machine Intelligence*, 19(7):757-763, 1997.
- [6] Hai Tao and Thomas S. Huang, "Facial animation and video tracking," *CAPTECH'98*, pages 242-253, 1998.
- [7] P. Kalra, A. Mangili, N. Magnenat-Thalmann, D. Thalmann, "Simulation of facial muscle actions based on rational free form deformations," *Proc. EUROGRAPHICS'92*, pages 59-69. Cambridge, 1992.
- [8] Koch R., Gross M., Carls F., Buren D., Fankhauser G. and Parish Y., "Simulating facial surgery using finite element models," *Proc. SIGGRAPH'96*, volume 30, pages 421-428. ACM, August 1996.
- [9] Kristinn R. Thórisson, "Gandalf: an embodied humanoid capable of real-time multimodal dialogue with people," *First ACM International Conference on Autonomous Agents*, 1997.
- [10] L. D. Landau and E. M. Lifshitz, *Theory of Elasticity*, Pergamon Press, London, UK, 1959.
- [11] Y. Lee, D. Terzopoulos, and K. Waters, "Realistic modeling for facial animation," *Proc. SIGGRAPH'95*, volume 30, pages 55-62. ACM, August 1995.
- [12] N. Magnenat-Thalmann, P. Kalra, M. Escher, "Face to virtual face," *Proceedings of the IEEE*, Vol. 86, No. 5, May 1998.
- [13] F. I. Parke, *Computer generated animation of faces*, Master's thesis, university of Utah, Salt Lake City, June 1972.
- [14] F. I. Parke, "Parameterized models for facial animation," *IEEE Computer Graphics and Application*, 2(9): 61-68, November 1982.
- [15] M. Patel and P. Willis, "FACES: The facial Animation, Construction and Editing System," *Eurographics'91*, pages 33-45, 1991.
- [16] W. H. Press, B. P. Fannery, S. A. Teukolsky, and W. T. Vetterling, *Numerical Recipes: The Art of Scientific Computing*, Cambridge University Press, Cambridge, UK, 1986.
- [17] D. Terzopoulos and K. Waters, "Analysis and synthesis of facial image sequences using physical and anatomical models," *IEEE Tran. Pattern Analysis and Machine Intelligence*, 15(6):569-579, June 1993.
- [18] P. L. Williams, R. Warwick, M. Dyson and L. H. Bannister, *Grey's Anatomy, 37th Edition*, Churchill Livingstone, London, 1989.
- [19] Y. Yacoob, Heung-Man Lam and Larry S. Davis, "Recognizing face showing expressions," *International Workshop on Automatic Face and Gesture Recognition*, Zurich, 1995.



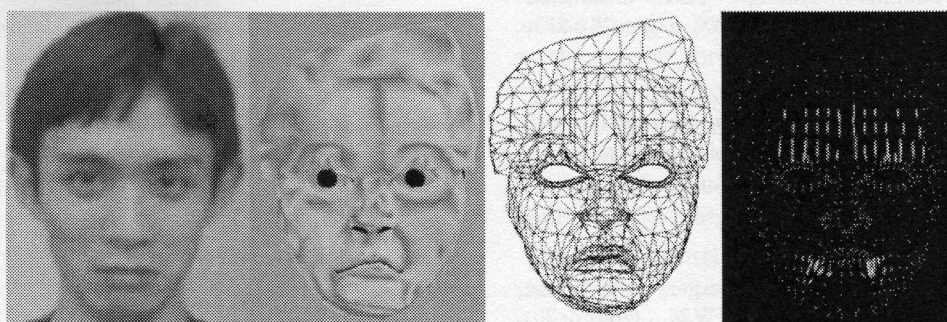
(a)



(b)



(c)



(d)

Figure 8: Synthesized primary facial expressions (a)Happiness (b)Anger (c)Surprise (d)Sadness